Mathematical Model of a Continuous Industrial High-Impact Polystyrene Process

Diana A. Estenoz and Gregorio R. Meira
Universidad Nacional del Litoral—CONICET, Güemes 3450, Santa Fe (3000), Argentina

Neidi Gómez and Haydée M. Oliva
Universidad del Zulia, Maracaibo, Venezuela

An industrial bulk process for the continuous production of high-impact polystyrene (HIPS) is mathematically modeled, and the model is validated with actual plant data. The steady states of two commercial HIPS grades were investigated. Polymer samples were taken along the process to measure monomer conversion, styrene (St) grafting efficiency, and free PS molecular weights. The model adequately reproduces the experimental measurements, and it also estimates the molecular macrostructure of the evolving reaction mixture.

Introduction

High-impact polystyrene (HIPS) is a composite material with rubber particles of around 2 μm dispersed in a vitreous polystyrene (PS) matrix. For optimal impact resistance properties, the rubber particles must be themselves heterogeneous, exhibiting typical "salami" structures, with vitreous microinclusions dispersed in the rubber. The influence of particle morphology on HIPS mechanical properties has been reported by Cigna et al. (1976), Aggarwal and Livigni (1977), Craig et al. (1977), Turley and Keskkula (1980), Hall et al. (1982), Mui et al. (1982), Hall (1988), Maestrini et al. (1992), Oliva et al. (1993), Oliva (1993), Anzaldi et al. (1994), Hazer and Kurt (1995), and Katime et al. (1995).

In the bulk HIPS process, styrene monomer (St) is polymerized in the presence of approximately 6% in weight of dissolved polybutadiene (PB) (Amos, 1974). Small amounts of other compounds such as a chemical initiator (to promote rubber grafting); a solvent (to lower viscosity); and a modifier (to lower molecular weights), may be also included in the recipe. The process is homogeneous up to about 2% conversion, and from then onwards it is heterogeneous. In the first part of the heterogeneous period, the continuous phase is rich in the rubber, while the disperse phase is rich in PS. Between 10 and 20% conversion, a phase inversion period occurs, and thereafter the vitreous matrix remains as the continuous phase. The graft copolymer tends to accumulate at the interfaces, favoring the development of the salami structure during the phase inversion, and in general stabilizing the heterogeneous mixture (both in the melt and in the final product).

A prepolymerization stage and a finishing stage can be distinguished in the bulk HIPS process. The prepolymerization lasts until around 30% conversion, and during this period the salami structure must be developed, since otherwise a low-value material is produced. For this reason, the prepolymerization is carried out under well-stirred conditions and in the presence of a chemical initiator. In the finishing stage, the polymerization mainly occurs by thermal monomer initiation, and mixing must be gentle to avoid destroying the salami structure. A devolatilization stage allows the solvent and the residual monomer to be eliminated. Typical final conversions of around 75% are reached.

In the recent article by Fischer and Hellmann (1996), the key role of the graft copolymer in the development of the salami morphology is highlighted. It was concluded that copolymer molecules with at least two grafts per molecule are necessary to make the external vitreous-rubber interface of the salami structure compatible, something copolymer molecules with only one graft cannot accomplish. These conclusions were made on the basis of a morphology analysis only, since no specific analytical method is as yet available to determine the number of grafted branches per molecule at different points of the heterogeneous structure.

Many experimental works have appeared on the synthesis

Correspondence concerning this article should be addressed to G. R. Meira.

and characterization of HIPS: for example, Brydon et al. (1973), Stein et al. (1975), Fischer (1973), Gasperowicz and Laskawski (1976), Kennedy and Delvaux (1981), Gupta et al. (1981), Sardelis et al. (1983), Solov'eva et al. (1983), Okamoto et al. (1991), Oliva et al. (1993), and Huang and Sundberg (1994). Purely theoretical works on the mathematical modeling of the HIPS synthesis are Brydon et al. (1974), Manaresi et al. (1975), Sundberg et al. (1984), Chern and Poehlein (1987), Estenoz and Meira (1993), and Huang and Sundberg (1995a). Finally, publications that contain both theoretical and experimental work on the HIPS synthesis are Tung and Wiley (1973), Ludwico and Rosen (1975), Peng (1990), Maestrini et al. (1992), Huang and Sundberg (1995b,c,d), Fischer and Hellmann (1996), and Estenoz et al. (1996a,b). Except for the early work by Ludwico and Rosen (1975), which does not consider the formation of graft copolymer, all other bulk-polymerization models produced so far ignore the inherent heterogeneity of the process, and assume a homogeneous reaction mixture. The homogeneous hypothesis was validated in several opportunities. For example, Fischer and Hellmann (1996) verified that the molecular characteristics and cast-film morphology of the polymer mixture produced in a solution polymerization are very similar to those obtained in an equivalent bulk polymerization.

Our previous publications in this series (Estenoz and Meira, 1993; Estenoz et al., 1996a,b) are unique in the sense that they calculate a detailed molecular macrostructure of the resulting graft copolymer. The kinetic mechanism in Estenoz et al. (1996a) assumes chemical initiation, thermal initiation, chain transfer to the rubber and to the monomer, propagation, termination by combination and disproportionation, and pure cross-linking between primary rubber radicals. The model in Estenoz et al. (1996a) also assumes a batch and homogeneous polymerization, the gel effect, and a reaction volume contraction. It enabled the calculation of the univariate-weight-molecular-weight distribution (WMWD) for the free PS and for the residual PB. Also, the complete bivariate WMWDs for the total graft copolymer and for each individual copolymer topology were estimated, with topologies classified according to the number of PS branches and PB chains per molecule. The model validation included published experimental data and ad hoc pilot plant experiments.

This work is the first attempt to model an industrial (continuous) HIPS process. The mathematical model of Estenoz et al. (1996a) is a point of departure of the present model that is verified against industrial measurements. Two stationary states (SS's) of a HIPS plant property of Estizulia C.A. (Maracaibo, Venezuela) were analyzed.

The experimental difficulties associated with the analysis of the evolving polymer mixture determined that only the free PS molecular weights could be measured. In contrast, the computer model allowed the detailed molecular macrostructure of each component in the evolving polymer mixture (i.e., PS, PB, and graft copolymer) to be predicted. The main limitations of the developed model are that it adopts the homogeneous hypothesis and that it does not include energy balances and mass-transfer phenomena. For this reason, other more "engineering" applications of the plant model, as for example, the evaluation of multiple steady states or the development of temperature control studies cannot at present be properly attempted.

Mathematical Model

Kinetic mechanism

In Table 1, the proposed kinetic mechanism is presented. It extends the mechanism in Estenoz et al. (1996a), by including a transfer reaction to a chain transfer agent (or "modifier"), and the deactivation of free radicals by an inhibitor (a catechol) that is not eliminated from the monomer. The employed symbols are explained in the Notation section. In the Detailed Kinetics column presented in the righthand-side of Table 1, copolymer species are classified according to

Table 1. The Adopted Kinetic Mechanism

Global Kinetics ($n, m = 1, 2, 3, \ldots$)	Detailed Kinetics ($s, s_1, s_2 = 0, 1, 2, \ldots$); ($b, b_1, n, m = 1, 2, 3, \ldots$)
Initiation	
$I_2 \xrightarrow{k_d} 2I^{\cdot}$	$I_2 \xrightarrow{k_d} 2I^{\cdot}$
$I^{\cdot} + St \xrightarrow{k_{i1}} S_1^{\cdot}$	$I^{\cdot} + St \xrightarrow{k_{i1}} S_1^{\cdot}$
$I^{\cdot} + P \xrightarrow{k_{i2}} P_0^{\cdot}$	$I^{\cdot} + P(s,b) \xrightarrow{k_{i2}} P_0^{\cdot}(s,b)$
Thermal initiation	
$3\,St \xrightarrow{k_{i0}} 2S_1^{\cdot}$	$3\,St \xrightarrow{k_{i0}} 2S_1^{\cdot}$
Propagation	
$S_n^{\cdot} + St \xrightarrow{k_p} S_{n+1}^{\cdot}$	$S_n^{\cdot} + St \xrightarrow{k_p} S_{n+1}^{\cdot}$
$P_0^{\cdot} + St \xrightarrow{k_{p0}} P_1^{\cdot}$	$P_0^{\cdot}(s,b) + St \xrightarrow{k_{p0}} P_1^{\cdot}(s,b)$
$P_n^{\cdot} + St \xrightarrow{k_p} P_{n+1}^{\cdot}$	$P_n^{\cdot}(s,b) + St \xrightarrow{k_p} P_{n+1}^{\cdot}(s,b)$
Transfer to the monomer	
$S_n^{\cdot} + St \xrightarrow{k_{fm}} S_n + S_1^{\cdot}$	$S_n^{\cdot} + St \xrightarrow{k_{fm}} S_n + S_1^{\cdot}$
$P_n^{\cdot} + St \xrightarrow{k_{fm}} P + S_1^{\cdot}$	$P_n^{\cdot}(s-n,b) + St \xrightarrow{k_{fm}} P(s,b) + S_1^{\cdot}$
$P_0^{\cdot} + St \xrightarrow{k'_{fm}} P + S_1^{\cdot}$	$P_0^{\cdot}(s,b) + St \xrightarrow{k'_{fm}} P(s,b) + S_1^{\cdot}$
Transfer to the PB or the copolymer	
$S_n^{\cdot} + P \xrightarrow{k_{fg}} S_n + P_0^{\cdot}$	$S_n^{\cdot} + P(s,b) \xrightarrow{k_{fg}} S_n + P_0^{\cdot}(s,b)$
$P_n^{\cdot} + P \xrightarrow{k_{fg}} P + P_0^{\cdot}$	$P_n^{\cdot}(s-n,b) + P(s_1,b_1) \xrightarrow{k_{fg}} P(s,b) + P_0^{\cdot}(s_1,b_1)$
Transfer to the modifier (X)	
$X + S_n^{\cdot} \xrightarrow{k_{fx}} S_1^{\cdot} + S_n$	$X + S_n^{\cdot} \xrightarrow{k_{fx}} S_1^{\cdot} + S_n$
$X + P_n^{\cdot} \xrightarrow{k_{fx}} S_1^{\cdot} + P$	$X + P_n^{\cdot}(s-n,b) \xrightarrow{k_{fx}} S_1^{\cdot} + P(s,b)$
$X + P_0^{\cdot} \xrightarrow{k'_{fx}} S_1^{\cdot} + P$	$X + P_0^{\cdot}(s,b) \xrightarrow{k'_{fx}} S_1^{\cdot} + P(s,b)$
Transfer to the inhibitor (Z)	
$Z + S_n^{\cdot} \xrightarrow{k_{fz}} Z^{\cdot} + S_n$	$Z + S_n^{\cdot} \xrightarrow{k_{fz}} Z^{\cdot} + S_n$
$Z + P_n^{\cdot} \xrightarrow{k_{fz}} Z^{\cdot} + P$	$Z + P_n^{\cdot}(s-n,b) \xrightarrow{k_{fz}} Z^{\cdot} + P(s,b)$
$Z + P_0^{\cdot} \xrightarrow{k'_{fz}} Z^{\cdot} + P$	$Z + P_0^{\cdot}(s,b) \xrightarrow{k'_{fz}} Z^{\cdot} + P(s,b)$
Termination by combination	
$S_n^{\cdot} + S_m^{\cdot} \xrightarrow{k_{tc}} S_{n+m}$	$S_n^{\cdot} + S_m^{\cdot} \xrightarrow{k_{tc}} S_{n+m}$
$P_m^{\cdot} + S_n^{\cdot} \xrightarrow{k_{tc}} P$	$P_{m-n}^{\cdot}(s-m,b) + S_n^{\cdot} \xrightarrow{k_{tc}} P(s,b)$
$P_m^{\cdot} + P_n^{\cdot} \xrightarrow{k_{tc}} P$	$P_{m-n}^{\cdot}(s-s_1-m,b-b_1) + P_n^{\cdot}(s_1,b_1) \xrightarrow{k_{tc}} P(s,b)$
$P_0^{\cdot} + P_n^{\cdot} \xrightarrow{k''_{tc}} P$	$P_0^{\cdot}(s-s_1-n,b-b_1) + P_n^{\cdot}(s_1,b_1) \xrightarrow{k''_{tc}} P(s,b)$
$P_0^{\cdot} + S_n^{\cdot} \xrightarrow{k''_{tc}} P$	$P_0^{\cdot}(s-n,b) + S_n^{\cdot} \xrightarrow{k''_{tc}} P(s,b)$
$P_0^{\cdot} + P_0^{\cdot} \xrightarrow{k'_{tc}} P$	$P_0^{\cdot}(s-s_1,b-b_1) + P_0^{\cdot}(s_1,b_1) \xrightarrow{k'_{tc}} P(s,b)$

their number of St and Bd repetitive units. From the Detailed Kinetics and after appropriate summations, the Global Kinetics can be restored.

In the mechanism of Table 1, the following was assumed: (a) intramolecular termination is neglected due to the extremely low probability that two free radicals can simultaneously occur in the same species; (b) all different types of $S_1^{\cdot}$ radicals react like a generic $S_n^{\cdot}$; (c) propagation, transfer, and termination by combination are unaffected by chain length; (d) termination by disproportionation is negligible at the employed temperatures; (e) the addition of an antioxidant mixture allows the high-temperature mechanisms of cross-linking, oxidation, and polymer degradation to be neglected; and (f) propagation reactions of the Bd double bonds to produce tetrafunctional PB-PS cross-links are neglected, as demonstrated by Chern and Poehlein (1987).

Both "T grafts" and "H grafts" are present in the graft copolymer. A T graft is generated when an St branch is linked onto a single PB chain by one end. An H graft is obtained when an St branch is linked onto two different PB chains by both ends. While H grafts are only produced by combination termination between copolymer radicals, T grafts are produced by transfer or inhibition of nonprimary copolymer radicals, and by combination termination between a PS homoradical and a (primary or nonprimary) rubber radical. Pure PB cross-links are obtained when two primary rubber radicals react together (last equation in Table 1). While T grafting does not alter the number of copolymer plus residual PB molecules, H grafting and pure PB cross-linking both reduce such number.

The homogeneous model

From the kinetics of Table 1, the mathematical model presented in the Appendix is obtained. The resulting model assumes a homogeneous polymerization, and it was developed for a generic continuous stirred-tank reactor (CSTR). The two nonagitated plant reactors were modeled as a series of five homogeneous CSTRs of the same total volume. The temperature was assumed to be known in each reactor, and its effect on the polymerization was introduced through the use of Arrhenius expressions in all kinetic constants. Also, the gel effect was indirectly taken into consideration by appropriately reducing the termination rate with increasing polymer volume fractions (Friis and Hamielec, 1976).

Equations A1–A3, A6–A9, A12, A15–A25, A28, A31–A33, A34, A37, A40, and A42–A46 in the Appendix constitute the final simulated model. To obtain the main global variables, such as conversion, concentration of initiator, monomer, and Bd double bonds, the subset of Eqs. A1–A3, A6–A9, A12, and A15–A25 must be initially solved. Then, the characteristics of the PS, the PB, and the graft copolymer can be independently calculated. For the PS and PB homopolymers, Eqs. A28 and A31–A33 must be respectively solved. For the graft copolymer, Eqs. A34, A37, A40, and A42–A46 are required. From the weight chain-length distributions (WCLDs) obtained through Eqs. A28, A31, and A40, then it is simple to calculate the corresponding WMWDs and averages. For example, from the PS and PB WCLDs represented by $G_{PS}(s)$ and $G_{PB}(b)$, the corresponding WMWDs $G_{PS}(M)$ and $G_{PB}(M)$ can be obtained by replacing the chain lengths s and b by the molecular weights $s\mathrm{M}_{St}$ and $b\mathrm{M}_{Bd}$. Similarly, from the graft copolymer bivariate distribution $G_C(s,b)$, the univariate WMWD $G_C(M)$, and chemical composition distribution $G_C(w_{St})$, are obtained, respectively, with the substitutions $M = s\mathrm{M}_{St} + b\mathrm{M}_{Bd}$ and $w_{St} = s\mathrm{M}_{St}/(s\mathrm{M}_{St} + b\mathrm{M}_{Bd})$, where w_{St} represents the weight fraction of St in the copolymer.

To calculate the WCLDs, a large number of differential equations must be simultaneously solved. In order to reduce such number, one possibility could have been to derive moment-based equations from Eqs. A28, A31, and A40; and to calculate the average chain lengths instead of the complete WCLDs. However, the complexity of the mentioned equations, and in particular of Eq. A40, makes such derivation practically impossible. The simplification method adopted in this work consisted of calculating a reduced number of (fictitious) molecular species, by lumping together all species that fall within fixed chain-length intervals. More specifically, 1,000 fictitious species were calculated for the free PS, adopting $\Delta s = 60$; 100 species were calculated for the unreacted PB, adopting $\Delta b = 200$; and 10,000 species were calculated for the graft copolymer, adopting $\Delta s = 600$ and $\Delta b = 200$.

Let us briefly consider the numerical solution of Eq. A40. In each calculation interval, all elements of the bivariate WCLD are simultaneously estimated. The first two terms in the righthand side of Eq. A40 represent the inlet and outlet molar flows of the (copolymer plus residual PB) species $\mathrm{P}(s,b)$; the third term represents the consumption of $\mathrm{P}(s,b)$ due to grafting and pure rubber cross-linking; the fourth to seventh terms represent the generation of $\mathrm{P}(s,b)$ due to T- and H-grafting; and the last term represents the generation of $\mathrm{P}(s,b)$ by pure rubber cross-linking. Except for the fourth to seventh terms, none of the other terms involve the generation of new branches, and are therefore relatively simple to implement. Consider in more detail the fourth to seventh terms, where m represents the chain length of the instantaneously grafted chains. The calculation procedure requires that first the chain-length distributions of the newly developed branches be estimated. Then, each of the species in such distributions are "distributed" among all species of the bivariate number chain-length distribution (NCLD) of $\mathrm{P}(s,b)$, according to their Bd contents. For example, in the fourth term of the righthand side of Eq. A40,

$$\left[R_p V(1-\varphi)\left(\tau - \gamma\tau_1 + \frac{\gamma\tau_1\varphi}{1-\varphi}\right)\alpha e^{-am}\right]$$

where $(m = 1, 2, \ldots)$ represents the NCLD of the new T branches produced by transfer reactions. For each m, the moles of the branches are first distributed among all the $\mathrm{P}(s,b)$ species according to their Bd contents, and then the newly resulting species are "relocated" in the bivariate NCLD of $\mathrm{P}(s,b)$. Finally, to produce the bivariate WCLD, the moles of $\mathrm{P}(s,b)$ must be multiplied by $(s\mathrm{M}_{St} + b\mathrm{M}_{Bd})$.

The model developed for a generic CSTR was sequentially applied along the reactor train to predict two SS operations and a transient evolution. For the SS calculations, all time derivatives were set to zero, and a standard procedure appropriate for nonlinear algebraic equations was applied. Also, each SS was obtained in a single calculation pass along the

reactor train, waiting for convergence in the first reactor before solving the second, and so on.

For the transients, the complete reactor train must be simultaneously solved, and the evolution of all intermediate variables and distributions must be stored. To integrate the large number of differential equations, a finite difference method that adopts a constant (but very small) time interval was applied. The time interval was selected with the criterion that further reductions in its value did not significantly alter the integration results. Through this procedure, highly accurate solutions (with errors lower than 0.01%) were obtained for the global predictions of Eqs. A1–A3, A6–A9, A12, and A15–A25.

For the chain-length distribution estimations, somewhat less accurate (but still satisfactory) predictions were obtained, in both the SS's and the transients. In the case of the PS and PB homopolymers, their chain-length intervals were reduced until differences lower than 0.1% were observed in the average chain lengths. In the case of the copolymer macrostructure, somewhat larger errors had to be admitted as a consequence of limitations in the computer memory. Thus, an error of 2% was observed in the number-average molecular weight of the copolymer obtained through Eq. A40 when compared with the more accurate value that can be derived from the results of Eqs. A1–A3, A6–A9, A12, and A15–A25. Finally, two independent checks were implemented to validate the WCLD results. First, it was verified that the masses under the WCLDs coincided with the masses predicted by Eqs. A1–A3, A6–A9, A12, and A15–A25. Second, it was verified that the SS solutions obtained after all transients had disappeared coincided with the independently obtained solutions via the nonlinear set of algebraic equations.

The computer program was written in FORTRAN for a 486 IBM-compatible PC. The total calculation times were approximately 2 min for solving an SS operation, and around 12 h for solving a transient calculation between two SS's. In both cases, most of those times were employed in calculating the copolymer bivariate distribution.

Experimental Work and Simulation Results

Industrial process

Figure 1 illustrates the investigated process. All tanks from R1 to R7 are considered reactors, since some polymerization is assumed to take place in each of them. In the devolatilizer R8, no initiation (and therefore no polymerization) can take place because the chemical initiator is completely consumed in R7, and the monomer is assumed to be totally stripped off from the polymer melt. Except for the initiator, all other reagents are dissolved and mixed in "reactor" R1. During the initial stage in R1 and R2, polymerization is in part inhibited by *tert*-butyl catechol, which is not eliminated from the monomer stock. The prepolymerization is carried out in reactors R3 and R4 (a train of two CSTRs); and the finishing stage takes place in reactors R5 and R6 (a train of two nonagitated reactors). For the devolatilization, the reaction mixture is first heated in R7 and then flashed under vacuum in R8. Polymer samples were taken at the points indicated with S2, S3, S4, S6, and S8 in Figure 1.

Two SS operations corresponding to the commercial grades PS4000 and PS4320 were analyzed. In Table 2, the feed conditions are presented. In the second and third columns of Tables 3 and 4, the reaction volumes (V) and the average temperatures (T) are given. For simplicity, V and T were held to be constant, while in reality they moderately oscillated around the given values. The main difference between the two grades is that a modifier and a larger PB concentration are included in the PS4320 recipe. The same base PB was employed in both experiments. The experimental WMWD of the initial PB is indicated by $G^0_{PB}(M)$ in Figure 2b and 2e. It was directly obtained from a set of 100 chromatogram points, and it should be noted that a linear scale was adopted for the molecular-weight axis. The PB microstructure indicated the following: 40% *cis*-1,4; 50% *trans*-1,4; and 10% 1,2 units.

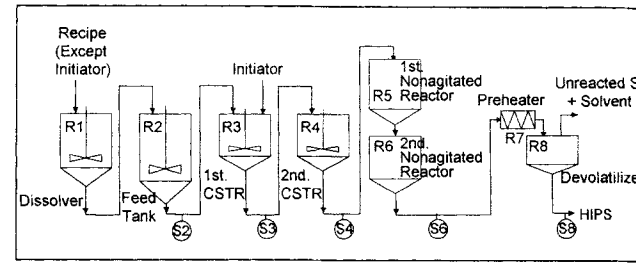

Figure 1. Investigated HIPS process.

The samples were analyzed to determine (a) monomer conversion (x); (b) the number- and weight-average molecular weights of the free PS ($\overline{M}_{n,PS}$ and $\overline{M}_{w,PS}$, respectively); and (c) the St grafting efficiency (E_{St}), defined as the percent of grafted St with respect to the total polymerized monomer. The measurements, corresponding to tanks R2, R3, R4, R6, and R8, are presented in the last five columns of Tables 3 and 4. As expected, PS molecular weights are lower in grade PS4320 than in PS4000.

Conversion was determined as follows. First, 10 g of reaction sample were dissolved in 35 mL of benzene containing hydroquinone as inhibitor. Then, all the polymer was precipitated in methanol and dried under vacuum at 60°C until constant weight. After subtraction of the original PB mass, the polymerized monomer mass and therefore conversion were calculated.

Table 2. Feed Conditions for the Two Investigated Grades

	PS4000	PS4320
Into Reactor 1		
Inlet Feed Flow; q^0_{in}	2.11×10^{-3} m^3/s	2.08×10^{-3} m^3/s
Feed stream density	870 kg/m^3	870 kg/m^3
Molar Concentrations		
Styrene; $[St]^0_{in}$	7,709 mol/m^3	7,495 mol/m^3
Butadiene repetititve units in PB; $[B^*]^0_{in}$	934 mol/m^3	1,166 mol/m^3
Modifier (*tert*-dodecyl mercaptane); $[X]^0_{in}$	0 mol/m^3	1.84 mol/m^3
Inhibitor (4-*tert*-butyl catechol); $[Z]^0_{in}$	0.079 mol/m^3	0.079 mol/m^3
Antioxidant mixture	3.293 mol/m^3	1.813 mol/m^3
Solvent (ethyl benzene)	880 mol/m^3	880 mol/m^3
Into Reactor 3		
Initiator inlet feed flow, q_I	1.9×10^{-6} m^3/s	2.2×10^{-6} m^3/s
Initiator molar concentration; $[I_2]^0_{in}$	981 mol/m^3	981 mol/m^3

Table 3. SS of Grade PS4000*

Reactor	Reaction Conditions		SS Results				
	V [m^3]	T [°C]	x [%]	E_{St} [%]	$\overline{M}_{n,PS}$ [g/mol]	$\overline{M}_{w,PS}$ [g/mol]	$\frac{\overline{M}_{w,PS}}{\overline{M}_{n,PS}}$
R1 (dissolver)	55.7	69	—	—	—	—	—
			0.5	1.4	704,000	134,000	1.91
R2 (feed tank)	79.1	65	**1.8**	—	—	—	—
			1.5	1.5	621,000	1,200,000	1.93
R3 (1st CSTR)	18.5	126	**27**	**6.9**	**117,000**	**267,000**	**2.28**
			28	6.1	117,000	262,000	2.24
R4 (2nd CSTR)	18.5	120	**40**	**5.3**	**128,000**	**292,000**	**2.28**
			37	6.0	124,000	272,000	2.19
R5 (1st nonagitated reactor)	22.9	141	—	—	—	—	—
			59	7.3	115,000	245,000	2.13
R6 (2nd nonagitated reactor)	5.50	168	**62**	**8.0**	**87,000**	**241,000**	**2.76**
			69	8.6	102,000	227,000	2.22
R7 (preheater)	0.484	238	—	—	—	—	—
			75	12.7	78,000	215,000	2.75
R8 (devolatilizer)	2.90	229	**76**	**14.2**	**79,000**	**224,000**	**2.85**
			75**	12.7**	78,000**	215,000**	2.75**

*Reactor conditions, experimental results (in bold), and corresponding theoretical predictions (in normal type).
**The predictions of R7 are repeated into R8, since no polymerization is assumed in the devolatilizer.

For the St grafting efficiency, a solvent extraction technique similar to that described in Peng (1990) was applied. The basic assumption was that all free PS was dissolved in a 50:50 methyl ethyl ketone/dimethylformamide (MEK/DMF) solvent mixture, while the copolymer and the PB homopolymer both remained insoluble. Unfortunately, the procedure is expected to provide estimations that are too large, due to the impossibility of completely extracting the free PS occluded in the rubber particles. This bias is in part compensated by the loss of low-molecular-weight copolymer that is washed out by the solvent. Also, the insolubles obtained at final conversion were partially cross-linked, thus further preventing the complete extraction of the occluded PS. For this reason, the errors in excess in E_{St} are expected to increase with conversion. The technique involved the following steps: (a) 0.200 ± 0.001 g of sample were loaded into 10 mL of MEK/DMF; (b) the mixture was agitated for 12 h and then centrifuged for 2 h at 12,000 rpm and 10°C; (c) the soluble

Table 4. SS of Grade PS4320*

Reactor	Reaction Conditions		SS Results				
	V [m^3]	T [°C]	x [%]	E_{St} [%]	$\overline{M}_{n,PS}$ [g/mol]	$\overline{M}_{w,PS}$ [g/mol]	$\frac{\overline{M}_{w,PS}}{\overline{M}_{n,PS}}$
R1 (dissolver)	64.0	59	—	—	—	—	—
			0.5	0.59	248,000	487,000	1.96
R2 (feed tank)	83.2	67	**1.8**	—	—	—	—
			1.7	0.72	234,000	460,000	1.96
R3 (1st CSTR)	17.7	122	**26**	**6.9**	**85,000**	**192,000**	**2.27**
			26	5.9	93,000	187,000	2.00
R4 (2nd CSTR)	18.5	125	**43**	**6.7**	**89,000**	**197,000**	**2.20**
			37	6.0	97,000	192,000	1.98
R5 (1st nonagitated reactor)	22.9	141	—	—	—	—	—
			59	7.2	91,000	179,000	1.98
R6 (2nd nonagitated reactor)	5.7	168	**69**	**8.1**	**75,000**	**170,000**	**2.20**
			69	8.8	82,000	168,000	2.05
R7 (preheater)	0.484	238	—	—	—	—	—
			74	11.4	70,000	161,000	2.30
R8 (devolatilizer)	2.89	227	**78**	**15.5**	**73,000**	**166,000**	**2.28**
			74**	11.4**	70,000**	161,000**	2.30**

*Reactor conditions, experimental results (in bold), and corresponding theoretical predictions (in normal type).
**The predictions of R7 are repeated into R8, since no polymerization is assumed in the devolatilizer.

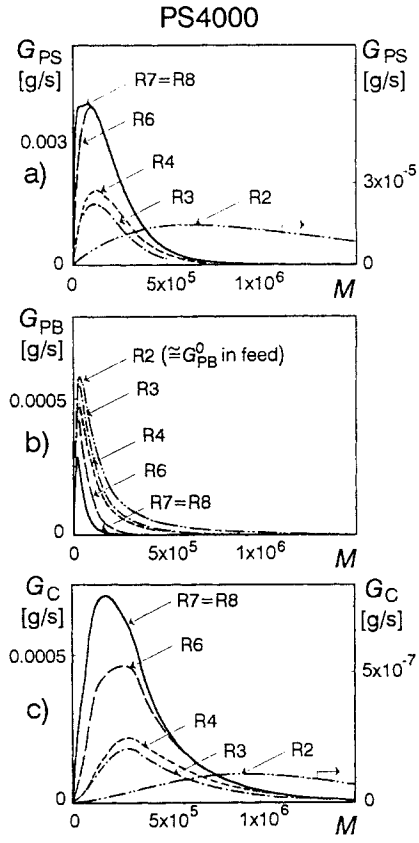

Figure 2. Predicted WMWDs obtained in the SS of grade PS4000, for reactors R2, R3, R4, R6, R7, and R8.

The molecular-weight axes are presented with a linear scale. In (b) the measured WMWD of the initial PB is shown. The area under the curves represents mass production. In (a) and (c) an amplified righthand-side scale is used for the distributions in R2.

portion was extracted; (d) the procedure was repeated with the addition of 10 mL more of the MEK/DMF mixture; (e) all PS solutions were mixed together, precipitated in methanol, and the insolubles dried under vacuum until constant weight; (f) the mass of grafted PS was determined by subtracting the initial PB mass from the insolubles weight; and (g) the St grafting efficiency was finally calculated.

For the molecular weight determinations, a Du Pont LC 870 size exclusion chromatograph, fitted with a UV detector and a set of PSM 60S and PSM 1000S Zorbax columns, was employed. The carrier solvent was tetrahydrofurane at 1.0 mL/min, and the temperature was controlled at 50°C.

Model Adjustment

In Table 5, the employed kinetic parameters are presented. The expressions for f, k_d, k_{fx}, k'_{fx}, k_{fz}, k'_{fz}, k_p, k_{tc}, k'_{tc}, and k''_{tc} were directly adopted from the literature; while k_{i0} and k_{fm} were adjusted within the ranges determined by the references. For k_{i2}, k_{fg}, and k_{fz} only indirect or incomplete literature values were found, and were therefore adjusted in this work. The adjustment was based on the SS of grade PS4000, since it involved a simpler kinetics. First, k_{i0} and k_{fm} were adjusted within literature ranges to fit the conversion and the PS molecular weights, respectively. Then, k_{fz} was adjusted with the knowledge that the inhibitor concentration was undetectable in R5, but still detectable in R4. Finally, k_{i2} and k_{fg} were adjusted to fit the St grafting efficiency during the prepolymerization and during the second half of the process, respectively. Finally, the measurements of grade PS4320 were verified. As can be seen in the last five columns of Tables 3 and 4, a reasonable overall agreement was obtained.

Discussion

All experimental and theoretical results on the investigated SS's are presented in Tables 3, 4, 6, and 7 and in Figures 2–4. Figure 5 contains the theoretical predictions of a transient between two SS's. Consider first the evolution of conversion (x) and of the St grafting efficiency (E_{St}) in Tables 3 and 4. In spite of the inhibitor, some polymerization still occurs in the dissolver and in the feed tank; and conversions over 1.5% were measured in R2. The predicted evolution of the inhibitor concentration $[Z]$ is shown in Tables 6 and 7. As can be seen in Tables 6 and 7, the concentration of primary rubber radicals $[P_0^{\cdot}]$ and consequently E_{St}, both increase in R3 due to the temperature increase and to the addition of the chemical initiator (I_2). The initiator is required to induce grafting during the prepolymerization. For this reason, its half-life is selected such that $[I_2]$ drops to negligible values after R4. During the second half of the process (the finishing and devolatilization stages) all reactions are thermally initiated. In R5 and R6, large increases in x and E_{St} are observed, due to the increased temperature and to the relatively large reaction volumes. The Preheater R7 exhibits a

Table 5. The Adopted Kinetic Constants

f		0.57	González et al., 1996
k_d	[s^{-1}]	$9.1\times10^{13}e^{-29,508/RT}$	González et al., 1996
$k_{tc}=k'_{tc}=k''_{tc}$	[L/(mol·s)]	$1.7\times10^{9}e^{-(1,667.3/RT)-2(c_1\psi+c_2\psi^2+c_3\psi^3)}$*	Friis and Hamielec, 1976
$k_p=k_{i1}^{**}=k_{p0}$**	[L/(mol·s)]	$1.0\times10^{7}e^{-7,067/RT}$	Villalobos et al., 1991
$k_{fx}=k'_{fx}$	[L/(mol·s)]	$6.0\times10^{6}e^{-6,640/RT}$	Brandrup and Immergut, 1989
$k_{fz}=k'_{fz}$	[L/(mol·s)]	$5.9\times10^{16}e^{-21,960/RT}$	Adjusted in this work
k_{i0}	[L^2/(mol^2·s)]	$1.1\times10^{5}e^{-27,340/RT}$	Peng, 1990; Yoon and Choi, 1995
$k_{fm}=k'_{fm}$	[L/(mol·s)]	$6.6\times10^{7}e^{-14,400/RT}$	Brandrup and Immergut, 1989
k_{i2}	[L/(mol·s)]	$2.0\times10^{6}e^{-7,067/RT}$	Adjusted in this work
k_{fg}	[L/(mol·s)]	$2.3\times10^{9}e^{-18,000/RT}$	Adjusted in this work

*$C_1=2.57-0.00505T$; $C_2=9.56-0.0176T$; $C_3=-3.03+0.00785T$; ψ = polymer volume fraction.
**Adopted equal to k_p, as suggested by Chern and Poehlein (1987).

Table 6. SS of Grade PS4000: More Theoretical Predictions

		Reactor						
		R1	R2	R3	R4	R5	R6	R7
q	[m^3/s]	2.11×10^{-3}	2.11×10^{-3}	2.02×10^{-3}	1.99×10^{-3}	1.93×10^{-3}	1.90×10^{-3}	1.89×10^{-3}
θ	[s]	26,400	37,500	9,160	9,300	11,900	2,900	256
[St]	[mol/m^3]	7,679	7,612	5,751	5,114	3,451	2,664	2,141
[B*]	[mol/m^3]	935	936	972	984	1,016	1,030	1,039
[I_2]	[mol/m^3]	0	0	1.57×10^{-2}	4.48×10^{-4}	6.55×10^{-13}	2.70×10^{-23}	5.04×10^{-27}
[Z]	[mol/m^3]	0.078	0.077	0.005	0.001	2.89×10^{-8}	5.07×10^{-14}	8.22×10^{-17}
[X]	[mol/m^3]	0	0	0	0	0	0	0
[S$^\cdot$]	[mol/m^3]	7.31×10^{-7}	9.71×10^{-7}	2.84×10^{-5}	1.17×10^{-5}	1.50×10^{-5}	2.26×10^{-5}	7.27×10^{-5}
[P$^\cdot$]	[mol/m^3]	7.26×10^{-9}	1.06×10^{-8}	1.35×10^{-6}	6.11×10^{-7}	1.77×10^{-6}	4.68×10^{-6}	3.15×10^{-5}
[$P_0^\cdot$]	[mol/m^3]	1.34×10^{-12}	2.32×10^{-12}	1.62×10^{-9}	4.62×10^{-10}	1.90×10^{-9}	8.93×10^{-9}	2.35×10^{-7}
G_{PS}	[g/s]	6.67	21.67	444.77	588.36	925.22	1,068.03	1,107.61*
G_{PB}	[g/s]	106.38	106.27	75.66	70.10	48.88	34.27	15.87*
G_C	[g/s]	0.14	0.48	59.65	73.88	130.04	171.37	251.68*
E_{PB}	[%]	0.04	0.14	28.90	34.13	54.07	67.80	85.09*
$\overline{M}_{n,PB}$	[g/mol]	71,500	71,500	57,400	54,700	44,200	36,800	27,300*
$\overline{M}_{w,PB}$	[g/mol]	296,000	295,000	180,000	159,000	102,000	75,000	52,500*
$\overline{M}_{w,PB}/\overline{M}_{n,PB}$	—	4.14	4.13	3.14	2.90	2.30	2.03	1.93*
$\overline{M}_{n,C}$	[g/mol]	1,080,000	983,000	357,000	366,000	344,000	313,000	256,000*
$\overline{M}_{w,C}$	[g/mol]	1,570,000	1,470,000	546,000	547,000	530,000	460,000	378,000*
$\overline{M}_{w,C}/\overline{M}_{w,C}$	—	1.45	1.50	1.53	1.49	1.54	1.47	1.48*
$\overline{w}_{St}$	[%]	72.49	69.89	48.60	51.06	55.79	57.93	59.56*
J_B	#/molec.	1.002	1.002	1.014	1.013	1.011	1.012	1.036*
$J_{S,T}$	#/molec.	0.998	0.998	1.359	1.379	1.588	1.888	3.280*
$J_{S,H}$	#/molec.	1.97×10^{-3}	2.07×10^{-3}	0.014	0.013	0.011	0.012	0.035*
J_X	#/molec.	5.07×10^{-14}	2.33×10^{-13}	1.13×10^{-8}	9.94×10^{-9}	1.08×10^{-8}	2.67×10^{-8}	2.66×10^{-6}*

*Coincident with the final outlet flow characteristics in R8.

Table 7. SS of Grade PS4320: More Theoretical Predictions

		Reactor						
		R1	R2	R3	R4	R5	R6	R7
q	[m^3/s]	2.08×10^{-3}	2.07×10^{-3}	2.00×10^{-3}	1.96×10^{-3}	1.90×10^{-3}	1.87×10^{-3}	1.86×10^{-3}
θ	[s]	26,400	37,500	9,160	9,300	11,900	2,900	256
[St]	[mol/m^3]	7,463	7,386	5,732	4,946	3,367	2,575	2,184
[B*]	[mol/m^3]	1,167	1,169	1,209	1,229	1,267	1,287	1,295
[I_2]	[mol/m^3]	0	0	2.70×10^{-2}	5.09×10^{-4}	6.67×10^{-13}	1.75×10^{-23}	5.83×10^{-27}
[Z]	[mol/m^3]	0.078	0.077	0.006	8.60×10^{-4}	2.72×10^{-8}	3.70×10^{-14}	1.09×10^{-16}
[X]	[mol/m^3]	1.83	1.82	1.40	1.21	0.83	0.64	0.55
[S$^\cdot$]	[mol/m^3]	7.02×10^{-7}	1.03×10^{-6}	2.91×10^{-5}	1.35×10^{-5}	1.46×10^{-5}	2.15×10^{-5}	5.97×10^{-5}
[P$^\cdot$]	[mol/m^3]	3.59×10^{-9}	6.80×10^{-9}	1.37×10^{-6}	7.33×10^{-7}	1.76×10^{-6}	5.01×10^{-6}	2.83×10^{-5}
[$P_0^\cdot$]	[mol/m^3]	1.65×10^{-12}	2.44×10^{-12}	2.19×10^{-9}	6.63×10^{-10}	1.54×10^{-9}	1.07×10^{-9}	2.66×10^{-7}
G_{PS}	[g/s]	8.06	27.36	396.67	563.89	887.70	1,020.26	1,063.00*
G_{PB}	[g/s]	130.93	130.81	93.78	85.09	64.58	62.65	26.67*
G_C	[g/s]	0.08	0.35	62.06	81.87	135.26	166.76	241.07*
E_{PB}	[%]	0.04	0.18	26.78	34.47	53.95	68.19	81.63*
$\overline{M}_{n,PB}$	[g/mol]	71,500	71,400	58,400	54,400	44,200	36,500	29,100*
$\overline{M}_{w,PB}$	[g/mol]	296,000	295,000	186,000	156,000	101,000	74,000	55,900*
$\overline{M}_{w,PB}/\overline{M}_{n,PB}$	—	4.14	4.13	3.18	2.86	2.29	2.03	1.92*
$\overline{M}_{n,C}$	[g/mol]	556,000	541,000	321,000	322,000	301,000	274,000	236,000*
$\overline{M}_{w,C}$	[g/mol]	920,000	899,000	507,000	499,000	446,000	378,000	319,000*
$\overline{M}_{w,C}/\overline{M}_{w,C}$	—	1.65	1.66	1.58	1.55	1.48	1.38	1.35*
$\overline{w}_{Si}$	[%]	46.76	45.39	41.39	44.01	49.24	52.23	53.74*
J_B	#/molec.	1.000	1.001	1.012	1.011	1.010	1.011	1.024*
$J_{S,T}$	#/molec.	1.000	1.000	1.311	1.352	1.564	1.879	2.691*
$J_{S,H}$	#/molec.	4.01×10^{-4}	5.40×10^{-4}	1.22×10^{-2}	1.08×10^{-2}	9.71×10^{-3}	1.07×10^{-2}	0.024*
J_X	#/molec.	7.04×10^{-14}	4.24×10^{-13}	1.45×10^{-8}	1.23×10^{-8}	1.36×10^{-8}	3.56×10^{-8}	1.33×10^{-6}*

*Coincident with the final outlet flow characteristics in R8.

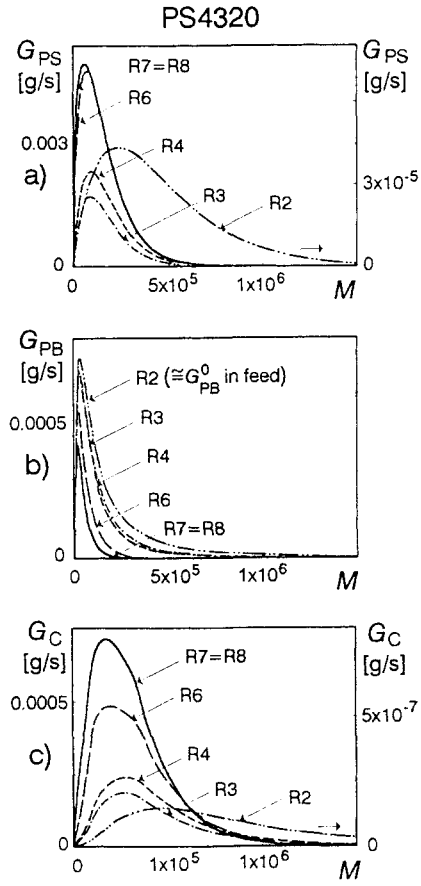

Figure 3. Predicted WMWDs obtained in the SS of grade PS4320, for reactors R2, R3, R4, R6, R7, and R8.

The molecular-weight axes are presented with a linear scale. In (b), the measured WMWD of the initial PB is shown. The area under the curves represents mass production. In (a) and (c), an amplified righthand-side scale is used for the distributions in R2.

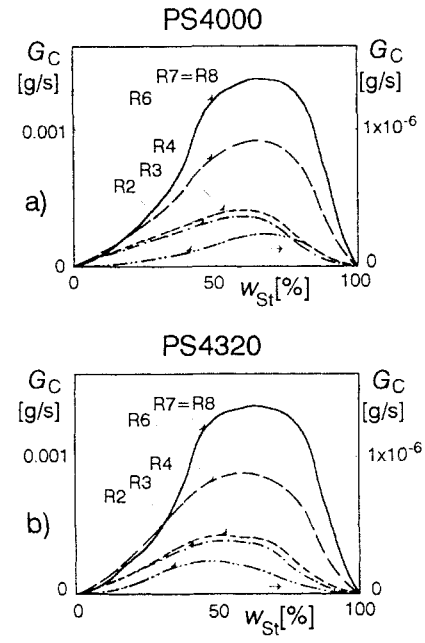

Figure 4. Predicted chemical composition distributions of the graft copolymer in reactors R2, R3, R4, R6, R7, and R8 for grade PS4000 (a), and for grade PS4320 (b).

Along the reactor train, the average copolymer composition first decreases and then increases. The area under the curves represents copolymer mass production. An amplified right-hand-side scale is employed for the distributions in R2.

small reaction volume but the highest process temperature, which favors further increases in x and E_{St}.

Consider the free PS molecular weights of Tables 3 and 4, Figures 2a and 3a. Unfortunately, only the average molecular weights were measured, and therefore the predicted WMWDs of Figures 2a and 3a could not be checked against measurements. In tanks R1 and R2, high molecular weights are produced because at the (lower) initial temperatures, most PS is generated by recombination termination. Even though produced in relatively small quantities, this initial high-molecular-weight fraction significantly affects the final $\bar{M}_{w,PS}$, and the final polydispersity $\bar{M}_{w,PS}/\bar{M}_{n,PS}$. PS molecular weights are largest in R1 and for grade PS4000, due to the absence of a modifier. During the prepolymerization in R3 and R4, PS molecular weights drop as a consequence of the chemical initiation and of the increased temperature that favors the transfer reactions to the monomer and to the modifier. In the second half of the process, PS molecular weights further decrease due to an even faster thermal initiation and transfer reactions. This determines that the final PS molecular weights are also the smallest, with a low-molecular-weight elbow appearing in the accumulated WMWDs, due to the low-molecular-weight polymer produced at high conversion (see Figures 2a and 3a).

The SS values of the total volume flow rate q, the residence time θ, and the reagent concentrations are presented in the first rows of Tables 6 and 7. The flow rate q decreases during the process due to volume contraction. A negligible consumption of Bd double bonds due to grafting is produced. This and the volume contraction determines an increase (rather than a decrease) in the concentration of unreacted

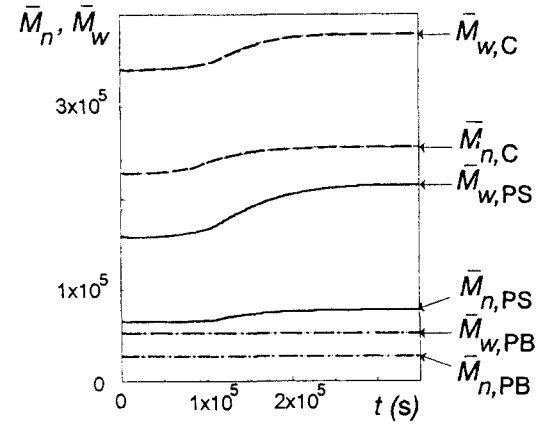

Figure 5. Time evolution of the average molecular weights in the final product after a step change from a theoretical SS of PS4320 to the experimental SS of PS4000.

Bd units [B*]. In grade PS4320, the modifier concentration [X] steadily drops along the process. In PS4320, the $\overline{M}_w$ values of the free PS and of the graft copolymer are systematically below those of PS4000.

Consider in Tables 6 and 7 the evolution of the outlet flow masses of PS, PB, and the copolymer (G_{PS}, G_{PB}, and G_C, respectively). Due to grafting, the final mass of PB plus graft copolymer is approximately 2.5 times the original PB mass for the grade PS4000, and approximately 2 times the original PB mass for PS4320. But since a smaller initial PB mass is incorporated into the PS4000 recipe, the mass fraction of total rubber in the final product is practically coincident in the two grades.

Consider the evolution of the unreacted PB presented in Tables 6 and 7, and in Figures 2b and 3b. PB molecular weights steadily drop as a consequence of the higher grafting probability of longer chains compared to shorter chains. For that same reason, $\overline{M}_{w,PB}$ drops faster than $\overline{M}_{n,PB}$. At final conversion, more than 80% of the original PB is transformed into graft copolymer. This is indicated by the PB grafting efficiency E_{PB}, defined as the ratio between the mass flow rate of grafted Bd chains and the mass flow rate of PB in the feed (Eq. A33). As expected, E_{PB} steadily increases during the process.

Graft copolymer predictions are presented in Tables 6 and 7, and in Figures 2c, 3c, and 4. Apart from the average molecular weights, the following averages are also presented: the global mass fraction of St ($\overline{w}_{St}$); the number of Bd chains per copolymer molecule (J_B); the number of T-grafted St chains per molecule ($J_{S,T}$); the number of H-grafted St chains per molecule ($J_{S,H}$); and the number of pure PB cross-links per molecule (J_X). The total number of Bd chains per molecule (J_B) and the total number of St chains per molecule ($J_S = J_{S,T} + J_{S,H}$) both must be ≥ 1. In R1 and R2, J_B and J_S are close to unity, thus indicating that the copolymer basically consists of the simplest T configuration. However, copolymer molecular weights are high in R1 and R2, because at the beginning of the process the longest Bd chains react first, and the grafted St branches are also the longest. During the prepolymerization, copolymer molecular weights drop due to chemical initiation and to the increased temperature (that favors chain transfer and thermal initiation). In PS4320, the values of the copolymer polydispersity $\overline{M}_{w,C}/\overline{M}_{n,C}$ and of the global composition $\overline{w}_{St}$ are systematically below those of PS4000. The main reason for this is that the St branches grafted to PS4320 are fewer and shorter than those grafted to PS4000. In effect, the copolymer is more highly grafted when the modifier is not included in the recipe; and while the final number of branches per molecule $J_B + J_S$ is approximately 4.4 for PS4000, that same variable is close to 3.7 for PS4320. Branching reactions increase at the (very high) preheater temperature, as indicated by the changes in J_B, $J_{S,T}$, $J_{S,H}$, and J_X, from R5 to R6.

According to predictions, the number of PB cross-links in the copolymer J_X always remains negligible in practice. The present computer model is incapable of predicting the ultrahigh molecular weights present in the insoluble gels that were observed in the final product. To calculate the gel fraction, a model modification that followed, for example, the "numerical fractionation" approach of Teymour and Campbell (1994) and of Ghielmi et al. (1996) could perhaps be attempted.

To test the dynamical model, a transient response between two SS's was simulated, but unfortunately no experimental measurements were taken to validate such predictions. The SS's could have coincided with the two investigated grades. However, this theory was discarded because the differences in the reactor volumes, the reactor temperatures, and the total feed flow into R1 introduced artificial step disturbances that are unrelated to the main mass balances. Instead, a theoretical initial SS for grade PS4320 was calculated, adopting the inlet concentrations into R1 of PS4320, and the reactor volumes, the temperatures, and the inlet flow into R1 of PS4000. From this theoretical SS, a transient was then calculated, assuming that at zero time, the inlet concentrations into R1 and the inlet feed of initiator into R3 were simultaneously changed to the values of the PS4000 recipe. It was verified that the SS obtained after the transient coincided with the SS for PS4000 independently calculated through the set of algebraic equations. Figure 5 shows the evolution of the average molecular weights observed in the final product for the graft copolymer and for the two homopolymers. The large residence times of reactors R1 and R2 determine a large induction time before noticeable variations in the molecular weights are observed. As expected, the transitions are smooth, and the global settling time is also in accord with the known plant behavior. The residual PB is seen to be practically unaffected by the change of grade.

Conclusions

The developed mathematical model (see the Appendix) estimates the total graft copolymer characteristics without resorting to the (more troublesome and inaccurate) calculation of the individual topologies, as in Estenoz et al. (1993, 1996a). The complex interrelationships between graft copolymer macrostructure, agitation, particle morphology, and the final mechanical properties is a challenging issue that is at present only beginning to be understood. In future communications, some of these aspects will be addressed.

In the present model, a homogeneous polymerization was assumed in spite of the two-phase nature of the process, and of the segregation that is to be expected at high conversion in the nonagitated reactors. However, good estimations of the measured variables were still obtained. This seems reasonable in the case of the free PS, since the main (thermally initiated) homopolymerization is expected to be little affected by the presence of the rubber. In the rubber phase, the homogeneous hypothesis may be introducing more serious errors, but such errors are at present impossible to evaluate, due to the difficulties associated with the isolation and analysis of the graft copolymer. With respect to the rubber products, only the total rubber mass (and the derived St grafting efficiency) could be measured with a relatively large error, indicating that most of the initial PB is transformed into graft copolymer. To fit the grafting efficiency measurements, two unknown kinetic constants (k_{i2} and k_{fg}) were adjusted. The parameter adjustment is clearly compensating for deviations from the homogeneous hypothesis. However, the procedure is at present justified by the necessity of developing a comprehensive model that provides a reasonable description of an industrial plant with a simplicity that is an asset in the complex kinetic of HIPS.

Acknowledgment

The authors thank Estizulia C.A. for its invaluable help regarding the two industrial experiments. Also, our CONICIT-CONICET international agreement, Universidad Nacional del Litoral, Universidad del Zulia, and CONDES-LUZ, are acknowledged for their financial support. Finally, our thanks to INDESCA (Venezuela) for the SEC measurements.

Notation

b = total repetitive units of Bd, dimensionless
Bd = butadiene
C = graft copolymer
c_j = mass concentration of j, with j = C, PB, or PS, mol/m^3
f = initiator efficiency, dimensionless
$G_j(M)$ = WMWD of j, with j = C, PB, or PS, g/s vs. g/mol
I$^\cdot$ = primary initiator radical
J_{PB} = average number of PB branches per copolymer molecule
k_d = initiator decomposition rate constant, s^{-1}
k_{fg} = rate constant of chain transfer to the rubber, L/(mol·s)
k_{fm}, k'_{fm} = rate constant of chain transfer to the monomer, L/(mol·s)
k_{fx}, k'_{fx} = rate constant of chain transfer to the modifier, L/(mol·s)
k_{fz}, k'_{fz} = rate constant of chain transfer to the inhibitor, L/(mol·s)
k_{i0} = rate constant of thermal monomer initiation, L^2/(mol^2·s)
k_{i1}, k_{i2}, k_{p0} = initiation rate constant, L/(mol·s)
k_p = propagation rate constant, L/(mol·s)
$k_{tc}, k'_{tc}, k''_{tc}$ = rate constant of recombination termination, L/(mol·s)
P = residual PB or copolymer molecule with (many) ungrafted Bd units
P$^\cdot$ = generic Bd radical
P$_0^\cdot(s,b)$ = primary rubber radical, generated from an attacked Bd unit of P(s,b)
P$_n^\cdot$ = nonprimary copolymer radical with a new growing branch containing n repetitive units of St
P$_n^\cdot(s,b)$ = P$_n^\cdot$ radical produced after a propagation of P$_0^\cdot(s,b)$
RI = Ith reactor
s = total repetitive units of St, dimensionless
S_n = PS molecule of chain length n
S$^\cdot$ = St radical
S$_n^\cdot$ = PS homoradical of chain length n
t = time, s
X = chain transfer agent
Z$^\cdot$ = stable radical
ψ = polymer volume fraction, dimensionless

Literature Cited

Aggarwal, S. L., and R. A. Livigni, "Structure and Properties of Microcomposites and Macrocomposites from Block Polymers," *Poly. Eng. Sci.*, **17**, 498 (1977).

Amos, J. L., "The SPE International Award Address—1973: The Development of Impact Polystyrene—A Review," *Poly. Eng. Sci.*, **14**, 1 (1974).

Anzaldi, S., L. Bonifaci, E. Malaguti, M. Vighi, and G. P. Ravanetti, "Some Considerations on the Second Phase Structure in High Impact Polystyrene and on the Related Measurement Methods," *J. Mat. Sci. Lett.*, **13**, 1555 (1994).

Brandrup, J., and E. H. Immergut, *Polymer Handbook*, 3rd ed., Wiley, New York (1989).

Brydon, A., G. M. Burnett, and G. G. Cameron, "Free-Radical Grafting of Monomers to Polydienes: I. Effect of Reaction Conditions on Grafting of Styrene to Polybutadiene," *J. Poly. Sci.*, **11**, 3255 (1973).

Brydon, A., G. M. Burnett, and G. G. Cameron, "Free-Radical Grafting of Monomers to Polydienes: II. Kinetics and Mechanism of Styrene Grafting to Polybutadiene," *J. Poly. Sci.*, **12**, 1011 (1974).

Chern, Ch. Sh., and G. W. Poehlein, "Kinetics of Grafting in Solution Polymerization," *Chem. Eng. Commun.*, **60**, 101 (1987).

Cigna, G., S. Matarrese, and G. F. Biglione, "Effect of Structure on Impact Strength of Rubber-Reinforced Polystyrene," *J. Appl. Poly. Sci.*, **20**, 2285 (1976).

Craig, T. O., R. M. Quick, and T. E. Jenkins, "Measurement of Particle Size Distribution in the Discrete Phase of High-Impact Polystyrene: II. An Improved Coulter Counter Procedure," *J. Poly. Sci.*, **15**, 441 (1977).

Estenoz, D. A., and G. R. Meira, "Grafting of Styrene onto Polybutadiene: Calculation of the Macrostructure," *J. Appl. Poly. Sci.*, **50**, 1081 (1993).

Estenoz, D. A., E. Valdez, H. M. Oliva, and G. R. Meira, "Bulk Polymerization of Styrene in Presence of Polybutadiene: Calculation of Molecular Macrostructure," *J. Appl. Poly. Sci.*, **59**, 861 (1996a).

Estenoz, D. A., G. P. Leal, Y. R. López, H. M. Oliva, and G. R. Meira, "Bulk Polymerization of Styrene in the Presence of Polybutadiene: The Use of Bifunctional Initiators," *J. Appl. Poly. Sci.*, **62**, 917 (1996b).

Friis, N., and A. E. Hamielec, "Gel-Effect in Emulsion Polymerization of Vinyl Monomers," *ACS Symp. Ser.*, **24**, 82 (1976).

Fischer, J. P., "Kinetic and Morphological Studies on the Free-Radical Grafting of Styrene on Polybutadienes," *Angew. Chem. Int. Ed.*, **12**, 428 (1973).

Fischer, M., and G. P. Hellmann, "On the Evolution of Phase Patterns during the High-Impact-Modified Polystyrene Process," *Macromol.*, **29**, 2498 (1996).

Gasperowicz, A., and W. Laskawski, "Grafting of Styrene onto Low Molecular Weight Polymers and Copolymers of Butadiene," *J. Poly. Sci.*, **14**, 2875 (1976).

Ghielmi, A., S. Fiorentino, G. Storti, M. Mazzotti, and M. Morbidelli, "Long Chain Branching in Emulsion Polymerization," *Int. Symp. on Free-Radical Polymerization*, Sta. Margherite Ligure, Italy (1996).

González, I. M., G. R. Meira, and H. Oliva, "Synthesis of Polystyrene with Mixtures of Mono- and Bifunctional Initiators," *J. Appl. Poly. Sci.*, **59**, 1015 (1996).

Gupta, V. K., G. S. Bhurgava, and K. K. Bhattacharyya, "Studies on Mechanism of Grafting of Polystyrene on Elastomer Backbone," *J. Macromol. Sci. Chem.*, A46(6), 1107 (1981).

Hall, R. A., R. D. Hites, and P. Plantz, "Characterization of Rubber Particle Size Distribution of High-Impact Polystyrene Using Low-Angle Laser Light Scattering," *J. Appl. Poly. Sci.*, **27**, 2885 (1982).

Hall, R. A., "Characterization of Rubber Particle Size Distribution of High-Impact Polystyrene Using an Image Analysis Method," *J. Appl. Poly. Sci.*, **36**, 1151 (1988).

Hazer, B., and A. Kurt, "Polymerization Kinetics of Styrene by Oligododecandioyl Peroxide, and Its Use in the Preparation of Graft Copolymers," *Eur. Poly. J.*, **31**, 499 (1995).

Huang, N. J., and D. C. Sundberg, "A Gel Permeation Chromatography Method to Determine Grafting Efficiency During Graft Copolymerization," *J. Appl. Poly. Sci.*, **35**(26), 5693 (1994).

Huang, N. J., and D. C. Sundberg, "Fundamental Studies of Grafting Reactions in Free Radical Copolymerization: I. A Detailed Kinetic Model for Solution Polymerization," *J. Appl. Poly. Sci.*, **33**, 2533 (1995a).

Huang, N. J., and D. C. Sundberg, "Fundamental Studies of Grafting Reactions in Free Radical Copolymerization: II. Grafting of Styrene, Acrylate, and Methacrylate Monomers onto *cis*-Polybutadiene Using AIBN Initiator in Solution Polymerization," *J. Appl. Poly. Sci.*, **33**, 2551 (1995b).

Huang, N. J., and D. C. Sundberg, "Fundamental Studies of Grafting Reactions in Free Radical Copolymerization: III. Grafting of Styrene, Acrylate, and Methacrylate Monomers onto *cis*-Polybutadiene Using Benzoyl Peroxide Initiator in Solution Polymerization," *J. Appl. Poly. Sci.*, **33**, 2571 (1995c).

Huang, N. J., and D. C. Sundberg, "Fundamental Studies of Grafting Reactions in Free Radical Copolymerization: IV. Grafting of Styrene, Acrylate, and Methacrylate Monomers onto Vinyl-Polybutadiene Using Benzoyl Peroxide and AIBN Initiators in Solution Polymerization," *J. Appl. Poly. Sci.*, **33**, 2587 (1995d).

Katime, A., J. Quintana, and C. Price, "Influence of the Microstructural Morphology on the Mechanical Properties of High-Impact Polystyrene," *Mat. Lett.*, **22**, 297 (1995).

Kennedy, J. P., and J. M. Delvaux, "Synthesis, Characterization and Morphology of Poly(Butadiene-g-Styrene)," *Adv. Poly. Sci.*, **38**, 141 (1981).
Ludwico, W. A., and S. L. Rosen, "The Kinetics of Two-Phase Bulk Polymerization: I. Monomer and Initiator Distribution," *J. Appl. Poly. Sci.*, **19**, 757 (1975).
Maestrini, C., M. Merlotti, M. Vighi, and E. Malaguti, "Second Phase Volume Fraction and Rubber Particle Size Determinations in Rubber-Toughened Polymers: A Simple Stereological Approach and Its Application to the Case of High Impact Polystyrene," *J. Mater. Sci.*, **27**, 5994 (1992).
Manaresi, V., V. Passalacqua, and F. Pilati, "Kinetics of Graft Polymerization of Styrene on *cis*-1-4-Polybutadiene," *Polymer*, **16**, 520 (1975).
Mui, E T. C., V. B. Boateng, J. F. Fullers, and J. L. White, "Interaction of Polymerization Conditions, Structural Variables, and Mechanical Properties of Rubber-Modified Plastics Produced from Bulk Polymerized Styrene/Poly(Butadiene-co-Styrene)," *J. Appl. Poly. Sci.*, **27**, 1395 (1982).
Okamoto, Y., H. Miyagi, and M. Kakugo, "Impact Improvement Mechanism of HIPS with Bimodal Distribution of Rubber Particle Size," *Macromol.*, **24**, 5639 (1991).
Oliva, H., G. Paricano, and J. Polo, "Efectos de Algunas Variables Operacionales Sobre las Propiedades Morfológicas y Mecánicas del Poliestireno de Alto Impacto," *Rev. Téc. Univ. Zulia (Venez.)*, **6**, 43 (1993).
Oliva, H., "Factores que Influyen Sobre las Propiedades del Poliestireno de Alto Impacto: Una Revisión," *Rev. Téc. Univ. Zulia (Venez.)*, **16**, 67 (1993).
Peng, F. M., "Polybutadiene Grafting and Crosslinking in High-Impact Polystyrene Bulk Thermal Process," *J. Appl. Poly. Sci.*, **40**, 1289 (1990).
Sardelis, K., H. J. Michelis, and G. Allen, "Toughened Polystyrene Containing High *cis*-1,4-Polybutadiene Rubber," *J. Appl. Poly. Sci.*, **28**, 3255 (1983).
Solov'eva, A. V., V. M. Bulotova, E. A. Egorova, E. A. Kirillova, and S. V. Kuznetsova, "Stabilisation of High-Impact PS during Synthesis," *Plasticheskie Massy.*, **9**, 13 (1983).
Stein, D. J., G. Fahrbach, and H. Addler, "Crosslinking Reaction in High Impact Polystyrene Rubber Particles," *Adv. Chem. Ser. (ACS)*, **142**, 148 (1975).
Sundberg, D. C., J. Arndt, and M. Y. Tang, "Grafting of Styrene onto Polybutadiene Lattices in Batch and Semi-Continuous Reactor," *J. Dispersion Sci. Technol.*, **5**, 433 (1984).
Teymour, F., and J. D. Campbell, "Analysis of the Dynamics of Gelation in Polymerization Reactors Using the Numerical Fractionation Technique," *Macromol.*, **27**, 2460 (1994).
Tung, L. H., and R. M. Wiley, "Random Grafting Statistics in Graft Distribution Analysis," *J. Poly. Sci., Poly. Phys. Ed.*, **11**, 1413 (1973).
Turley, S. G., and H. Keskkula, "Effect of Rubber-Phase Volume Fraction in Impact Polystyrene on Mechanical Behaviour," *Polymer*, **21**, 466 (1980).
Villalobos, M. A., A. E. Hamielec, and P. E. Wood, "Kinetic Model for Short-Cycle Bulk Styrene Polymerization through Bifunctional Initiators," *J. Appl. Poly. Sci.*, **42**, 629 (1991).
Yoon, W. J., and K. Y. Choi, "Kinetics of Free-Radical Styrene Polymerization with the Symmetrical Bifunctional Initiator 2,5-Dimethyl-2,5-Bis(2-Ethyl Hexanoyl Peroxy)Hexane," *Polymer*, **33**(21), 4582 (1992).

Appendix: Mathematical Model for a Generic CSTR

Global kinetics module

The following mass balances can be written on the basis of the global kinetics in Table 1.

Initiator.

$$\frac{d}{dt}\{[I_2]V\} = \begin{cases} q_I[I_2]^0_{in} - q[I_2] - k_d[I_2]V & \text{for reactor R3} \\ q_{in}[I_2]_{in} - q[I_2] - k_d[I_2]V & \text{for reactors R4–R7,} \end{cases} \quad \text{(A1)}$$

where [ ] indicates molar concentration in mol/m^3; the superscript 0 denotes feed stock condition; V is the reaction volume in m^3; q_I is the initiator feed flow into reactor R3 in m^3/s; q_{in} and q are the total inlet and outlet flow rates in m^3/s; and subscript in denotes the inlet condition.

Monomer. Assuming the "long chain approximation" (by which propagation is the only monomer consuming reaction), we can write

$$\frac{d}{dt}\{[St]V\} = q_{in}[St]_{in} - q[St] - R_pV \quad \text{(A2)}$$

with

$$R_p = k_p([S^\cdot] + [P^\cdot])[St] \quad \text{(A3)}$$

$$[S^\cdot] = \sum_{n=1}^{\infty} [S_n^\cdot] \quad \text{(A4)}$$

$$[P^\cdot] = \sum_{n=1}^{\infty} [P_n^\cdot] \quad \text{(A5)}$$

where R_p is the global rate of St consumption in mol/(m$^3\cdot$s) and $[S^\cdot]$ and $[P^\cdot]$ are the global concentrations of $S_n^\cdot$ and $P_n^\cdot$ radicals, respectively.

Modifier.

$$\frac{d}{dt}\{[X]V\} = q_{in}[X]_{in} - q[X] - \{k_{fx}([S^\cdot] + [P^\cdot]) + k'_{fx}[P_0^\cdot]\}[X]V. \quad \text{(A6)}$$

Inhibitor.

$$\frac{d}{dt}\{[Z]V\} = q_{in}[Z]_{in} - q[Z] - \{k_{fz}([S^\cdot] + [P^\cdot]) + k'_{fz}[P_0^\cdot]\}[Z]V. \quad \text{(A7)}$$

Unreacted Bd Units. Let us represent with B* any unreacted Bd unit present in the copolymer or in the initial (or purely cross-linked) PB. When a P molecule is attacked, a B* unit is consumed; and when a $P_0^\cdot$ radical terminates, a B* unit is regenerated. Thus:

$$\frac{d}{dt}\{[B^*]V\} = q_{in}[B^*]_{in} - q[B^*] - \{k_{i2}[I^\cdot] + k_{fg}([S^\cdot] + [P^\cdot])\}[B^*]V + \{k'_{fm}[St] + k'_{fx}[X] + k'_{fz}[Z]\}[P_0^\cdot]V. \quad \text{(A8)}$$

Radical Species. The balance of the free radicals together with the pseudo-steady-state assumption yields:

$$\frac{d}{dt}\{[I^{\cdot}]V\} = q_{in}[I^{\cdot}]_{in} - q[I^{\cdot}] + \{2fk_d[I_2] - (k_{i1}[St] + k_{i2}[B^*])[I^{\cdot}]\}V \cong 0 \quad \text{(A9)}$$

$$\frac{d}{dt}\{[S_1^{\cdot}]V\} = q_{in}[S_1^{\cdot}]_{in} - q[S_1^{\cdot}] + k_{i1}[I^{\cdot}][St]V + 2k_{i0}[St]^3V + (k_{fm}[St] + k_{fx}[X])([S^{\cdot}] + [P^{\cdot}])V + (k'_{fm}[St] + k'_{fx}[X])[P_0^{\cdot}]V - \{k_p[St] + k_{fg}[B^*] + k_{fm}[St]\}[S_1^{\cdot}]V - \{k_{fx}[X] + k_{fz}[Z] + k''_{tc}[P_0^{\cdot}] + k_{tc}([S^{\cdot}] + [P^{\cdot}])\} \times [S_1^{\cdot}]V \cong 0 \quad \text{(A10)}$$

$$\frac{d}{dt}\{[S_n^{\cdot}]V\} = q_{in}[S_n^{\cdot}]_{in} - q[S_n^{\cdot}] + k_p[St][S_{n-1}^{\cdot}]V - \{k_p[St] + k_{fm}[St] + k_{fx}[X]\}[S_n^{\cdot}]V - \{k_{fz}[Z] + k_{fg}[B^*] + k''_{tc}[P_0^{\cdot}] + k_{tc}([S^{\cdot}] + [P^{\cdot}])\}[S_n^{\cdot}]V \cong 0, \quad n = 1,2,3,\ldots \quad \text{(A11)}$$

$$\frac{d}{dt}\{[P_0^{\cdot}]V\} = q_{in}[P_0^{\cdot}]_{in} - q[P_0^{\cdot}] + \{k_{i2}[I^{\cdot}] + k_{fg}([S^{\cdot}] + [P^{\cdot}])\} \times [B^*]V - \{k_{p0}[St] + k'_{fm}[St] + k'_{fx}[X] + k'_{fz}[Z] + k'_{tc}[P_0^{\cdot}] + k''_{tc}([S^{\cdot}] + [P^{\cdot}])\}[P_0^{\cdot}]V \cong 0 \quad \text{(A12)}$$

$$\frac{d}{dt}\{[P_1^{\cdot}]V\} = q_{in}[P_1^{\cdot}]_{in} - q[P_1^{\cdot}] + k_{p0}[St][P_0^{\cdot}]V - (k_p + k_{fm})[St][P_1^{\cdot}]V - \{k_{fx}[X] + k_{fz}[Z] + k_{fg}[B^*] + k''_{tc}[P_0^{\cdot}] + k''_{tc}([S^{\cdot}] + [P^{\cdot}])\}[P_1^{\cdot}]V \cong 0 \quad \text{(A13)}$$

$$\frac{d}{dt}\{[P_n^{\cdot}]V\} = q_{in}[P_n^{\cdot}]_{in} - q[P_n^{\cdot}] + k_p[St][P_{n-1}^{\cdot}]V - (k_p + k_{fm})[St][P_n^{\cdot}]V - \{k_{fx}[X] + k_{fz}[Z] + k_{fg}[B^*] + k''_{tc}[P_0^{\cdot}] + k''_{tc}([S^{\cdot}] + [P^{\cdot}])\}[P_n^{\cdot}]V \cong 0, \quad n = 1,2,3,\ldots. \quad \text{(A14)}$$

Adding Eq. A10 with Eq. A11 over all n's, and Eq. A13 with Eq. A14 over all n's, results in:

$$\frac{d}{dt}\{[S^{\cdot}]V\} = q_{in}[S^{\cdot}]_{in} - q[S^{\cdot}] + k_{i1}[St][I^{\cdot}]V + 2k_{i0}[St]^3V + (k'_{fm}[St] + k'_{fx}[X])[P_0^{\cdot}]V + (k_{fm}[St] + k_{fx}[X])[P^{\cdot}]V - \{k_{fg}[B^*] + k''_{tc}[P_0^{\cdot}] + k''_{tc}([S^{\cdot}] + [P^{\cdot}])\}[S^{\cdot}]V \cong 0 \quad \text{(A15)}$$

$$\frac{d}{dt}\{[P^{\cdot}]V\} = q_{in}[P^{\cdot}]_{in} - q[P^{\cdot}] + k_{p0}[St][P_0^{\cdot}]V - k_{fm}[St][P^{\cdot}]V - \{k_{fx}[X] + k_{fz}[Z] + k_{fg}[B^*] + k''_{tc}([S^{\cdot}] + [P^{\cdot}])\}[P^{\cdot}]V \cong 0. \quad \text{(A16)}$$

Volume and Conversion. Define conversion x by

$$x = \frac{q_{in}^0[St]_{in}^0 - q[St]}{q_{in}^0[St]_{in}^0}. \quad \text{(A17)}$$

Assuming a simple St homopolymerization with a constant rubber volume, we can write:

$$\frac{dV}{dt} = q_{in} - q, \quad \text{(A18)}$$

with

$$q = q_{in} - q_{St,in}\epsilon(x_{in} - x), \quad \text{(A19)}$$

where $\epsilon = 0.137$ is the (dimensionless) volume contraction factor corresponding to PS homopolymer; x_{in} is the inlet conversion; and $q_{St,in}$ is the inlet St flow rate. By adopting constant reaction volumes, Eq. A18 may be set equal to zero.

In order to solve all previous balances, Eqs. A1–A3, A6–A9, A12, and A15–A19 must be simultaneously integrated.

WCLD of the Free PS. Define first the following dimensionless parameters:

$$\varphi = \frac{[S^{\cdot}]}{[S^{\cdot}] + [P^{\cdot}]} \quad \text{(A20)}$$

$$\beta = \frac{k_{tc}R_p}{(k_p[St])^2} \quad \text{(A21)}$$

$$\tau = \frac{k_{fm}}{k_p} + \frac{k_{fx}[X]}{(k_p[St])} + \frac{k_{fz}[Z]}{(k_p[St])} + \frac{k_{fg}[B^*]}{(k_p[St])} + \gamma\tau_1 \quad \text{(A22)}$$

$$\tau_1 = \frac{k''_{tc}R_p}{(k_p[St])^2} \quad \text{(A23)}$$

$$\gamma = \frac{[P_0^{\cdot}]}{[S^{\cdot}] + [P^{\cdot}]} \quad \text{(A24)}$$

$$\alpha = \tau + \beta. \quad \text{(A25)}$$

To calculate the WCLD of the accumulated free PS, the following mass balances must be written:

$$\frac{d}{dt}\{[S_n]V\} = q_{in}[S_n]_{in} - q[S_n] + (k_{fm}[St] + k_{fx}[X] + k_{fz}[Z] + k_{fg}[B^*]) \times [S_n^{\cdot}]V + \frac{k_{tc}}{2}\sum_{m=1}^{n-1}[S_m^{\cdot}][S_{n-m}^{\cdot}]V, \quad n = 1,2,3,\ldots. \quad \text{(A26)}$$

Considering Eqs. A3, A10, A11, A15, and A20–A25, and operating as in Estenoz et al. (1996a), the following can be obtained:

$$\frac{d}{dt}\{[S_n]V\} = q_{in}[S_n]_{in} - q[S_n] + \left[R_pV\varphi(\tau-\gamma\tau_1) + \frac{R_pV\varphi^2\beta}{2}\alpha n\right]\alpha e^{-\alpha n}, \quad n=1,2,3,\ldots. \tag{A27}$$

To calculate the WCLD of the free PS, let us multiply each of Eqs. A27 by the corresponding molecular weights (nM_{St}), yielding:

$$\frac{d}{dt}\{c_{PS}(n)V\} = q_f c_{PS}(n)_f - qc_{PS}(n) + \left[R_pV\varphi(\tau-\gamma\tau_1) + \frac{R_pV\varphi^2\beta}{2}\alpha n\right]\alpha M_{St} n e^{-\alpha n}, \quad n=1,2,3,\ldots, \tag{A28}$$

where c indicates mass concentration in g/m^3. Representing the free PS production per unit time in g/s by G, then the WCLD is obtained from $G_{PS}(n) = qc_{PS}(n)$.

WCLD of the Unreacted PB. In the global kinetics of Table 1, P represents both the accumulated copolymer and the residual PB. Consider only the reactions involving the unreacted PB and the reactions at each possible chain length, b. Calling $[n_{PB}(n)]$ the molar concentration of unreacted PB species of chain length n, then $b[n_{PB}(b)]$ is the molar concentration of B* at each chain length. Assuming that the number of attacked B* units is proportional to the B* contents of each chain-length class, then the fraction of $P_0^{\cdot}$ radicals that are primary PB radicals of chain length b is $\{b[n_{PB}(b)]/[B^*]\}$. Thus, with a treatment similar to that in Estenoz et al. (1996a), the following can be obtained:

$$\frac{d}{dt}\{[n_{PB}(b)]V\} = q_{in}[n_{PB}(b)]_{in} - q[n_{PB}(b)] - \{k_{i2}[I^{\cdot}] + k_{fg}([S^{\cdot}]+[P^{\cdot}])\}b[n_{PB}(b)]V + \{k'_{fx}[X] + k'_{fz}[Z] + k'_{fm}[St]\}[P_0^{\cdot}]\frac{b[n_{PB}(b)]V}{[B^*]}, \quad b=1,2,3,\ldots. \tag{A29}$$

Introducing Eqs. A3, A12, A16, and A20–A25 into Eq. A29, results in:

$$\frac{d}{dt}\{[n_{PB}(b)]V\} = q_{in}[n_{PB}(b)]_{in} - q[n_{PB}(b)] - \left\{R_pV(1-\varphi)\left(\tau-\gamma\tau_1+\beta\varphi+\frac{\gamma\tau_1\varphi}{1-\varphi}\right) + R_pV(1-\varphi) \times\left[\beta(1-\varphi)+2\gamma\tau_1 + \frac{R_p^2\gamma^2Vk'_{tc}}{(k_p[St])^2}\right\}\frac{b[n_{PB}(b)]}{[B^*]}, \quad b=1,2,3,\ldots. \tag{A30}$$

Multiplying each of Eqs. A30 by their corresponding molecular weights (bM_{Bd}), we get:

$$\frac{d}{dt}\{c_{PB}(b)V\} = q_{in}c_{PB}(b)_{in} - qc_{PB}(b) - \left\{R_pV(1-\varphi)\left(\tau-\gamma\tau_1+\beta\varphi+\frac{\gamma\tau_1\varphi}{1-\varphi}\right) + R_pV(1-\varphi) \times[b(1-\varphi)+2\gamma\tau_1] + \frac{R_p^2\gamma^2Vk'_{tc}}{(k_p[St])^2}\right\}\frac{bc_{PB}(b)}{[B^*]}, \quad b=1,2,3,\ldots, \tag{A31}$$

where c indicates mass concentration in g/m^3.

Finally, the WCLD of the unreacted PB is given by $G_{PB}(b) = qc_{PB}(b)$, with G representing the unreacted PB mass per unit time, in g/s.

Global Derived Variables. From the previous results, the St grafting efficiency (E_{St}) and the PB grafting efficiency (E_{PB}) can be calculated from:

$$E_{St} = \frac{xq_{in}^0[St]_{in}^0 - \sum_n G_{PS}(n)}{xq_{in}^0[St]_{in}^0} \tag{A32}$$

and

$$E_{PB} = \frac{\sum_b G_{PB}^0(b)_{in} - \sum_b G_{PB}(b)}{\sum_b G_{PB}^0(b)_{in}}, \tag{A33}$$

where $G_{PB}^0(b)$ is the WCLD of the initial PB.

Detailed kinetics module or copolymer quality equations

Bivariate Copolymer Distribution. Let us represent with $B^*(s,b)$ any unreacted Bd unit of $P(s,b)$. From the detailed kinetics of Table 1, the mass balances for every possible radical species (together with the pseudo-steady-state assumption) yields:

$$\frac{d}{dt}\{[P_0^{\cdot}(s,b)]V\} = q_{in}[P_0^{\cdot}(s,b)]_{in} - q[P_0^{\cdot}(s,b)] + \{k_{i2}[I^{\cdot}] + k_{fg}([S^{\cdot}]+[P^{\cdot}])\}[B^*]V + \{k_{p0}[St] + k'_{fm}[St] + k'_{fx}[X] + k'_{fz}[Z] + k'_{tc}[P_0^{\cdot}] + k''_{tc}([S^{\cdot}]+[P^{\cdot}])\} \times[P_0^{\cdot}(s,b)]V \cong 0, \quad s=0,1,2,\ldots; \quad b=1,2,3,\ldots. \tag{A34}$$

$$\frac{d}{dt}\{[P_1^{\cdot}(s,b)]V\} = q_{in}[P_1^{\cdot}(s,b)]_{in} - q[P_1^{\cdot}(s,b)] + k_{p0}[St][P_0^{\cdot}(s,b)]V - (k_p + k_{fm})[St][P_1^{\cdot}(s,b)]V - \{k_{fx}[X] + k_{fz}[Z] + k_{fg}[B^*] + k''_{tc}[P_0^{\cdot}] + k_{tc}([S^{\cdot}]+[P^{\cdot}])\} \times[P_1^{\cdot}(s,b)]V \cong 0, \quad s=0,1,2,\ldots; \quad b=1,2,3,\ldots. \tag{A35}$$

$$\frac{d}{dt}\{[P_n^{\cdot}(s,b)]V\} = q_{in}[P_n^{\cdot}(s,b)]_{in} - q[P_n^{\cdot}(s,b)] + k_p[St][P_{n-1}^{\cdot}(s,b)]V - (k_p + k_{fm})[St][P_n^{\cdot}(s,b)]V - \{k_{fx}[X] + k_{fz}[Z] + k_{fg}[B^*] + k_{tc}''[P_0^{\cdot}] + k_{tc}([S^{\cdot}] + [P^{\cdot}])\} \times [P_n^{\cdot}(s,b)] \cong 0, \quad s = 0,1,2,\ldots; \quad b = 1,2,3,\ldots. \tag{A36}$$

Comparing Eqs. A12 and A34, we find:

$$\frac{[P_0^{\cdot}(s,b)]}{[P_0^{\cdot}]} = \frac{[B^*(s,b)]}{[B^*]}, \quad s = 0,1,2,\ldots; \quad b = 1,2,3,\ldots. \tag{A37}$$

Equation A37 confirms the assumption adopted in Eq. A29, that the fraction of primary radicals generated from $P(s,b)$ (with respect to the total number of primary rubber radicals), coincides with the molar fraction of unreacted B* units in each species (with respect to the total B* units).

The bivariate WCLD for the accumulated copolymer can be obtained from the following mass balance:

$$\frac{d}{dt}\{[P(s,b)]V\} = q_{in}[P(s,b)]_{in} - q[P(s,b)] + T_1 + T_2 + T_3 + T_4 + T_5, \quad s,b = 1,2,3,\ldots, \tag{A38a}$$

with

$$T_1 = -[B^*(s,b)]\{k_{i2}[I^{\cdot}] + k_{fg}([S^{\cdot}] + [P^{\cdot}])\}V \tag{A38b}$$

$$T_2 = (k_{fm}[St] + k_{fx}[X] + k_{fz}[Z] + k_{fg}[B^*]) \times \sum_{m=1}^{s} [P_m^{\cdot}(s-m,b)]V + k_{tc}\sum_{m=2}^{s}\sum_{n=1}^{m-1}[P_n^{\cdot}(s-m,b)][S_{m-n}^{\cdot}]V + k_{tc}''\sum_{m=1}^{s}[P_0^{\cdot}(s-m,b)][S_m^{\cdot}]V \tag{A38c}$$

$$T_3 = \frac{k_{tc}}{2}\sum_{b_1=1}^{b-1}\sum_{s_1+m=2}^{s}\sum_{n=1}^{m-1}[P_{m-n}^{\cdot}(s-s_1,b-b_1)] \times [P_n^{\cdot}(s_1,b_1)]V + \sum_{b_1=1}^{b-1}\sum_{s_1+m=2}^{s}k_{tc}''[P_m^{\cdot}(s-s_1-m,b-b)] \times [P_0^{\cdot}(s_1,b_1)]V \tag{A38d}$$

$$T_4 = \{k_{fm}'[St] + k_{fx}'[X] + k_{fz}'[Z]\}[P_0^{\cdot}(s,b)]V \tag{A38e}$$

$$T_5 = \frac{k_{tc}'}{2}\sum_{b_1=1}^{b-1}\sum_{s_1=1}^{s}[P_0^{\cdot}(s-s_1,b-b_1)][P_0^{\cdot}(s_1,b_1)]V, \tag{A38f}$$

where T_1 represents the rate of disappearance of the accumulated $P(s,b)$ by generation of $P_0^{\cdot}(s,b)$; T_2 represents the rate of generation of $P(s,b)$ by grafting of a new T branch of length m onto a $P(s-m,b)$ species; T_3 represents the rate of generation of $P(s,b)$ by linking $P(s-s_1-m,b-b_1)$ and $P(s-s_1,b-b_1)$ with a new H branch of length m; T_4 represents the rate of regeneration of $P(s,b)$ by deactivation of primary $P_0^{\cdot}(s,b)$ radicals; and T_5 represents the rate of generation of $P(s,b)$ copolymer by direct cross-linking between $P_0^{\cdot}(s-s_1,b-b_1)$ and $P_0^{\cdot}(s_1,b_1)$.

Following similar treatment as in Estenoz et al. (1996a), Eqs. A3, A12, A16, A20–A25, and A33–A37 may be introduced into Eqs. A38, resulting in

$$\frac{d}{dt}\{[P(s,b)]V = q_{in}[P(s,b)]_{in} - q[P(s,b)] - \left\{\left[R_pV(1-\varphi)\left(\tau - \gamma\tau_1 + \beta\varphi + \frac{\gamma\tau_1\varphi}{1-\varphi}\right)\right] + [R_pV(1-\varphi)(\beta(1-\varphi)+2\gamma\tau_1)] + \left[\frac{R_p^2V\gamma^2k_{tc}''}{(k_p[St])^2}\right]\right\}\frac{[B^*(s,b)]}{[B^*]} + R_pV(1-\varphi)\left(\tau - \gamma\tau_1 + \frac{\gamma\tau_1\varphi}{1-\varphi}\right)\sum_{m=1}^{s}\frac{[B^*(s-m,b)]}{[B^*]} \times \alpha e^{-\alpha m} + R_pV\varphi(1-\varphi)\beta\sum_{m=1}^{s}\frac{[B^*(s-m,b)]}{[B^*]}\alpha^2me^{-\alpha m} + R_pV(1-\varphi)\gamma\tau_1\sum_{b_1=1}^{b-1}\sum_{s_1+m=1}^{s}\frac{[B^*(s-s_1-m,b-b_1)]}{[B^*]} \times \frac{[B^*(s_1,b_1)]}{[B^*]}\alpha e^{-\alpha m} + R_pV(1-\varphi)^2\frac{\beta}{2}\sum_{b_1=1}^{b-1}\sum_{s_1+m=1}^{s} \times \frac{[B^*(s-s_1-m,b-b_1)]}{[B^*]} \times \frac{[B^*(s_1,b_1)]}{[B^*]}\alpha^2me^{-\alpha m} + \frac{R_p^2V\gamma^2k_{tc}''}{2(k_p[St])^2}\sum_{b_1=1}^{b-1}\frac{[B^*(s-s_1,b-b_1)]}{[B^*]} \times \frac{[B^*(s_1,b_1)]}{[B^*]}, \quad s,b = 1,2,3,\ldots. \tag{A39}$$

Multiplying Eqs. A39 by the molecular weights of each copolymer class $(sM_{St} + bM_{Bd})$, the WCLD for the total copolymer can be obtained:

$$\frac{d}{dt}\{c_C(s,b)V\} = q_{in}c_C(s,b)_{in} - qc_C(s,b) - \left\{\left[R_pV(1-\varphi)\left(\tau - \gamma\tau_1 + \beta\varphi + \frac{\gamma\tau_1\varphi}{1-\varphi}\right)\right] + [R_pV(1-\varphi)(\beta(1-\varphi)+2\gamma\tau_1)] + \left[\frac{R_p^2V\gamma^2k_{tc}''}{(k_p[St])^2}\right]\right\}\frac{[B^*(s,b)]}{[B^*]} \times (sM_{St} + bM_{Bd}) + R_pV(1-\varphi)\left(\tau - \gamma\tau_1 + \frac{\gamma\tau_1\varphi}{1-\varphi}\right) \times \sum_{m=1}^{s}\frac{[B^*(s-m,b)]}{[B^*]}\alpha e^{-\alpha m}(sM_{St} + bM_{Bd}) + R_pV\varphi(1-\varphi)\beta\sum_{m=1}^{s}\frac{[B^*(s-m,b)]}{[B^*]}\alpha^2me^{-\alpha m} \times (sM_{St} + bM_{Bd}) + R_pV(1-\varphi)\gamma\tau_1$$

$$\times \sum_{b_1=1}^{b-1} \sum_{s_1+m=1}^{s} \frac{[B^*(s-s_1-m,b-b_1)]}{[B^*]} \frac{[B^*(s_1,b_1)]}{[B^*]} \alpha e^{-\alpha m}$$

$$\times (sM_{St}+bM_{Bd}) + R_pV(1-\varphi)^2 \frac{\beta}{2} \sum_{b_1=1}^{b-1} \sum_{s_1+m=1}^{s}$$

$$\times \frac{[B^*(s-s_1-m,b-b_1)]}{[B^*]} \frac{[B^*(s_1,b_1)]}{[B^*]} \alpha^2 m e^{-\alpha m}$$

$$\times (sM_{St}+bM_{Bd}) + \frac{R_p^2 V \gamma^2 k''_{tc}}{2(k_p[St])^2} \sum_{b_1=1}^{b-1} \frac{[B^*(s-s_1,b-b_1)]}{[B^*]}$$

$$\times \frac{[B^*(s_1,b_1)]}{[B^*]} (sM_{St}+bM_{Bd}), \quad s,b=1,2,3,\ldots, \quad \text{(A40)}$$

where c indicates mass concentration in g/m^3.

After solving the global kinetics module, the simultaneous solution of Eqs. A34, A37, and A40 allows us to obtain $c_C(s,b)$. From $c_C(s,b)$, the bivariate WCLD $G_C(s,b)=q\,c_C(s,b)$ may be calculated, where G is the copolymer mass produced per unit time, in g/s.

Comparing Eqs. A40 with Eqs. A31, it is easy to prove that the latter is a special case of the first where $s=0$. In effect, in the case of unreacted PB, T_2, T_3, and T_5 in Eqs. A40 are all zero, since PB molecules are basically consumed (and eventually only generated by deactivation of a primary PB radical).

Average Number of St Branches per Copolymer Molecule. The third term on the righthand side of Eq. A39 can be written as follows:

$$T = \left\{ \left[R_pV(1-\varphi)\left(\tau - \gamma\tau_1 + \beta\varphi + \frac{\gamma\tau_1\varphi}{1-\varphi}\right)\right] + [R_pV(1-\varphi)(\beta(1-\varphi)+2\gamma\tau_1)] + \left[\frac{R_p^2V\gamma^2k''_{tc}}{(k_p[St])^2}\right]\right\} \times \frac{[B^*(s,b)]}{[B^*]} = N_I \times \frac{[B^*(s,b)]}{[B^*]}. \quad \text{(A41)}$$

In Eq. A41, N_I represents the rate of generation of new grafting points or of primary $P_0^{\cdot}(s,b)$ radicals, while $[B^*(s,b)]/[B^*]$ "distributes" such grafting points among the accumulated $P(s,b)$ species proportionately to their B* contents. In turn, N_I is made up of three terms. The first term represents the rate of generation of new T grafting sites; the second term represents the rate of generation of new H grafting sites; and the third term represents the rate of consumption of active sites by direct cross-linking of two Bd radicals without St intervention.

One St branch is incorporated per T graft, while two St branches are incorporated per H graft. The mass balances for the number of T- and H-grafted St branches $J_{S,T}$ and $J_{S,H}$, respectively, can be "extracted" from Eq. A39, yielding:

$$\frac{d\{J_{S,T}V/q\}}{dt} = J_{S,T_{in}} - J_{S,T} + \left[R_pV(1-\varphi)\left(\tau-\gamma\tau_1+\beta\varphi+\frac{\gamma\tau_1\varphi}{1-\varphi}\right)\right] \Big/ \sum_{b=1}^{\infty}\sum_{s=1}^{\infty}[P(s,b)]V \quad \text{(A42)}$$

$$\frac{d\{J_{S,H}V/q\}}{dt} = J_{S,H_{in}} - J_{S,H} + \frac{1}{2}[R_pV(1-\varphi)(\beta(1-\varphi)+2\gamma\tau_1)] \Big/ \sum_{b=1}^{\infty}\sum_{s=1}^{\infty}[P(s,b)]V. \quad \text{(A43)}$$

Average Number of Pure Cross-Links per Copolymer Molecule. Calling J_X the number of pure cross-links per copolymer molecule, the following balances can also be "extracted" from Eq. A39:

$$\frac{d\{J_XV/q\}}{dt} = J_{X_{in}} - J_X + \left[\frac{R_p^2V\gamma^2k''_{tc}}{(k_p[St])^2}\right] \Big/ \sum_{b=1}^{\infty}\sum_{s=1}^{\infty}[P(s,b)]V. \quad \text{(A44)}$$

Global Copolymer Composition. The global mass fraction of St in the copolymer can be obtained from:

$$\overline{w}_{St} = \frac{\sum_{b=1}^{\infty}\sum_{s=1}^{\infty} sM_{St}[P(s,b)]}{\sum_{b=1}^{\infty}\sum_{s=1}^{\infty}(sM_{St}+bM_{Bd})[P(s,b)]}. \quad \text{(A45)}$$

Average Number of PB Branches per Copolymer Molecule. After solving Eqs. A30 and A39, the number of PB branches per copolymer molecule may be calculated as follows:

$$J_{PB} = \frac{\sum_{s=1}^{\infty}[n^0_{PB}(b)]_{in}q^0_{in} - \sum_{s=1}^{\infty}[n_{PB}(b)]q}{\sum_{b=1}^{\infty}\sum_{s=1}^{\infty}[P(s,b)]q}. \quad \text{(A46)}$$

Manuscript received Nov. 4, 1996, and revision received Sept. 24, 1997.